

Self-assembly and magnetic properties of shape-controlled monodisperse $\text{Co Fe}_2\text{O}_4$ nanocrystals

Ningzhong Bao, Liming Shen, Prahallad Padhan, and Arunava Gupta

Citation: [Applied Physics Letters](#) **92**, 173101 (2008); doi: 10.1063/1.2917444

View online: <http://dx.doi.org/10.1063/1.2917444>

View Table of Contents: <http://scitation.aip.org/content/aip/journal/apl/92/17?ver=pdfcov>

Published by the [AIP Publishing](#)

Articles you may be interested in

[Anisotropic strain, magnetic properties, and lattice dynamics in self-assembled multiferroic \$\text{CoFe}_2\text{O}_4\text{-PbTiO}_3\$ nanostructures](#)

J. Appl. Phys. **115**, 134317 (2014); 10.1063/1.4870803

[Magneto-optic material selectivity in self-assembled \$\text{BiFeO}_3 - \text{CoFe}_2\text{O}_4\$ biferroic nanostructures](#)

J. Appl. Phys. **105**, 07C124 (2009); 10.1063/1.3074099

[Synthesis, structure, and magnetic studies on self-assembled \$\text{Bi Fe O}_3 - \text{Co Fe}_2\text{O}_4\$ nanocomposite thin films](#)

J. Appl. Phys. **103**, 07E301 (2008); 10.1063/1.2832346

[Self-assembled multiferroic nanostructures in the \$\text{Co Fe}_2\text{O}_4 - \text{Pb Ti O}_3\$ system](#)

Appl. Phys. Lett. **87**, 072909 (2005); 10.1063/1.2031939

[Magnetic properties of self-assembled interacting nanoparticles](#)

Appl. Phys. Lett. **81**, 4574 (2002); 10.1063/1.1528290



Self-assembly and magnetic properties of shape-controlled monodisperse CoFe_2O_4 nanocrystals

Ningzhong Bao, Liming Shen, Prahallad Padhan, and Arunava Gupta^{a)}

Center for Materials for Information Technology, University of Alabama, Tuscaloosa, Alabama 35487, USA

(Received 15 March 2008; accepted 7 April 2008; published online 28 April 2008)

Ordered arrays of monodisperse cobalt ferrite (CoFe_2O_4) nanocrystals with highly controllable spherical or cubic shapes have been synthesized via solution-based thermolysis of an intimately mixed $\text{Co}^{2+}\text{Fe}_2^{3+}$ -oleate precursor. The evolution from spherical to cubic morphology is achieved by simply changing the precursor concentration, thereby controlling the nanocrystal growth rate. Magnetic studies indicate that the saturation magnetization is independent of the shape and is solely determined by the size of the nanocrystal. However, the coercivity does exhibit a small shape dependence, primarily resulting from the influence of surface anisotropy. © 2008 American Institute of Physics. [DOI: 10.1063/1.2917444]

Ordered arrays of monodisperse nanocrystals with controlled shapes and sizes have gained importance in recent years in the fields of materials chemistry and physics.¹⁻³ Nanometer-sized materials, including nanotubes, nanorods, nanowires, nanocubes, etc, exhibit a wide range of optical, electrical, magnetic, and catalytic properties that are highly shape dependent.^{1,2} A number of materials, including metals, alloys, binary oxides and chalcogenides, and some ternary compounds have thus far been investigated.^{1,2} In addition to their individual characteristics, the monodisperse nanocrystals can serve as building blocks for the fabrication of thin films and other functional systems, with applications in the field of data storage, spintronics, solar cell, sensor, catalysis, etc.^{1,2,4} For data storage and spintronic applications, it is desirable to develop strategies for the self-assembly of thin films of shape-controlled magnetic nanocrystals, in particular, the complex metal oxides that display a wide range of properties of practical interest.⁵

The spinel ferrites of composition $M\text{Fe}_2\text{O}_4$ ($M=\text{Co}, \text{Ni}, \text{Mn}, \text{Fe}, \text{etc.}$) exhibit interesting magnetic, magnetoresistive, and magneto-optical properties that are potentially useful for a broad range of applications.⁶ Their magnetic properties can be systematically varied by changing the identity of the divalent M^{2+} cation or by partial substitution while maintaining the basic crystal structure.⁷ The magnetic properties can additionally be tuned by controlling the shape of the nanocrystals since the shape can influence the anisotropic magnetic properties. Indeed, variations in the magnetic anisotropy have been observed in cubic and polyhedron-shaped MnFe_2O_4 nanoparticles prepared by a seed-mediated growth process involving thermal decomposition of mixed $\text{Mn}^{2+}-\text{Fe}^{3+}$ acetylacetonates in a high boiling-point solvent with added surfactants.⁸ As one of the intensively investigated ferrites, cobalt ferrite (CoFe_2O_4) with an inverse spinel structure is well known to have a relatively large magnetic anisotropy, moderate saturation magnetization, remarkable chemical stability, and mechanical hardness. The seed-mediated growth process has been previously utilized for the preparation of monodisperse, shape-controlled CoFe_2O_4 nanoparticles.^{9,10}

In order to avoid the use of toxic and expensive organometallic compounds, such as iron pentacarbonyl, an attractive alternative for the thermolytic synthesis of a wide range of binary metal oxides is the use of metal-oleate complexes prepared by reacting relatively inexpensive and environmentally friendly metal chloride and sodium oleate precursors.^{11,12} With adequate choice of oleates that have similar decomposition temperatures and are intimately mixed, we have recently extended the process to the synthesis of ternary $M\text{Fe}_2\text{O}_4$ ($M=\text{Co}, \text{Ni}, \text{Mn}, \text{and Fe}$) ferrite nanocrystals.¹³ Herein, we report on the direct synthesis of monodisperse spherical and cubic CoFe_2O_4 nanocrystals by merely changing the concentration of the starting $\text{Co}^{2+}\text{Fe}_2^{3+}$ -oleate precursor. We achieve shape control by taking advantage of the fact that the growth of elongated non-spherical nanocrystals requires a higher concentration of the precursors in the solution. Additionally, we have investigated the shape-dependent magnetic properties of the CoFe_2O_4 nanocrystals.

In a typical synthesis, 20 mmol FeCl_3 , 10 mmol CoCl_2 , 82.5 mmol sodium oleate, 40 ml H_2O , 45 ml ethanol, and 90 ml hexane were mixed and refluxed at 60 °C for 4 h. The intimately mixed $\text{Co}^{2+}\text{Fe}_2^{3+}$ -oleate complex mixture was obtained by separation of the water phase and evaporation of the residual water, ethanol, and hexane from the solution. Monodisperse ~12 nm spherical and ~17 nm cubic CoFe_2O_4 nanocrystals were obtained by thermolysis of 3 and 6 g, respectively, of the $\text{Co}^{2+}\text{Fe}_2^{3+}$ -oleate complex dissolved in 20 ml of 1-octadecene at 320 °C for 1 h under N_2 flow. After reaction, the size distribution of the nanocrystals is further reduced by centrifugation and the nanocrystals are then dried in an oven at 35 °C. A small quantity (about 15 mg) of the dried CoFe_2O_4 powder is used for the magnetic measurements, while a dilute solution of the dispersed powder in hexane is used for the microscopy studies.

Phase identification and the degree of crystallinity of the products have been studied by using powder x-ray diffraction (XRD). The typical XRD patterns of both the spherical [Fig. 1(a)] and cubic CoFe_2O_4 nanocrystals [Fig. 1(b)] show strong but relatively broad diffraction peaks that can be indexed to the spinel CoFe_2O_4 phase without any evidence of preferential crystallographic orientation. No additional or intermediate phase is detected in the products. The average

^{a)} Author to whom correspondence should be addressed. Electronic mail: agupta@mint.ua.edu.

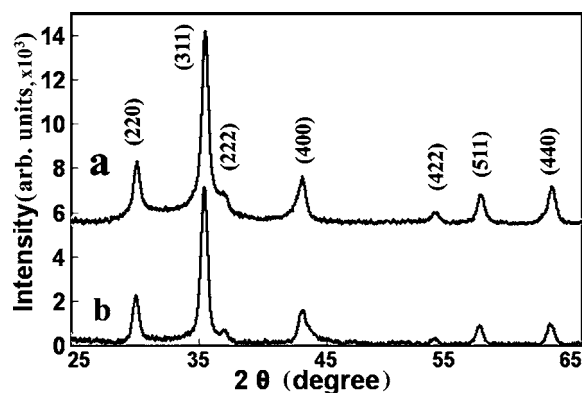


FIG. 1. XRD patterns of (a) spherical and (b) cubic CoFe_2O_4 nanocrystals.

crystalline sizes estimated using the Scherrer formula are 12.5 and 13.8 nm for the spherical and cubic nanocrystals, respectively, based on the width of (311) peak.

It is interesting to note that the shape of the CoFe_2O_4 nanocrystals can be tuned from spherical to cubic shape solely by increasing the concentration of the synthetic precursors. Figures 2(a)–2(d) show the transmission electron microscopy (TEM) and high resolution TEM (HRTEM) images of the spherical (11.2 ± 0.4 nm) and the cubic nanocrystals (11.5 ± 0.5 nm), respectively. The observed sizes for both shapes agree well with those estimated from the XRD results. Both types of nanocrystals exhibit a narrow size distribution and, depending on the concentration of the nanocrystals in solution, form ordered arrays of monolayer films [Figs. 2(a)–2(d)]. The HRTEM images [the insets to Figs. 2(b) and 2(d)] of the various CoFe_2O_4 nanocrystals show clear lattice fringes corresponding to a group of atomic planes, indicating their single crystalline nature. The shape and the size of the synthesized nanocrystals are determined by two related factors—the magic size nuclei and the con-

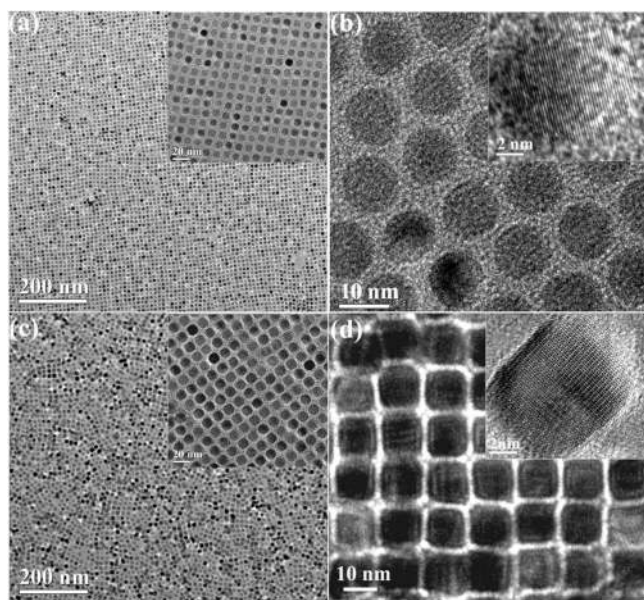


FIG. 2. Large- and small-area TEM images of [(a) and (b)] 11.2 ± 0.4 nm spherical and [(c) and (d)] 11.5 ± 0.4 nm cubic CoFe_2O_4 nanocrystals, showing highly ordered CoFe_2O_4 nanocrystal arrays. The insets to (b) and (d) are HRTEM images of individual spherical or cubic CoFe_2O_4 nanocrystals showing the crystal lattice fringes, indicating the single crystalline nature of the CoFe_2O_4 nanocrystals.

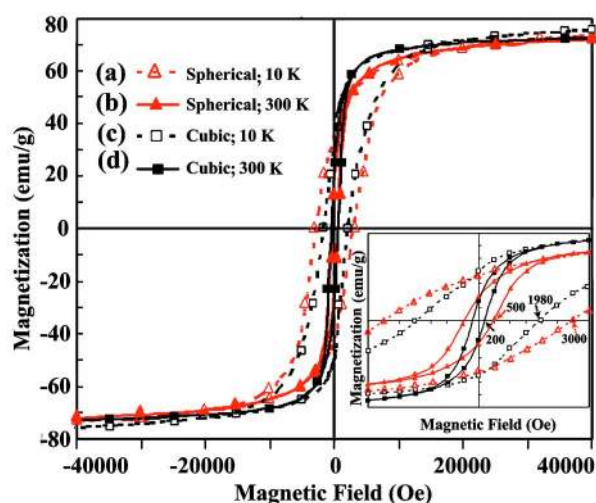


FIG. 3. (Color online) Magnetic hysteresis loops of spherical CoFe_2O_4 nanocrystals measured at (a) 10 K (b) 300 K and cubic CoFe_2O_4 nanocrystals measured at (c) 10 K (d) 300 K. The inset shows enlarged magnetic hysteresis loops at low applied fields, more clearly displaying the coercivity of the samples.

centration of the residual synthetic precursor monomers after the initial nucleation stage. A higher monomer concentration in solution is basically required for the growth of elongated nanocrystals, such as the cubic nanocrystals.^{1,14} The yields of the perfectly spherical and cubic nanocrystals shown in Fig. 2 are essentially 100%. In contrast to the synthesis procedure of the cubic nanocrystals, a reduction of the aging time to 10 min at 320 °C results in the formation of primarily the cubic-shaped product with yield of over 90% and a few spherical, spherical-to-cubic, near-cubic, and edge-grown cubic-shaped nanoparticles (not shown). The existence of these intermediate-shaped nanocrystals provides support for the initial formation of spherical nanocrystals with subsequent growth to form mostly the cubic shape nanocrystals.

The hysteresis loops of the different shaped CoFe_2O_4 nanocrystals have been measured by using a superconducting quantum interference device at 10 and 300 K. The magnetization curves, as shown in Fig. 3, display relatively high saturation magnetization. The saturation magnetization values of the spherical and cubic CoFe_2O_4 nanocrystals are 72.9 and 73.3 emu/g, respectively, measured at 300 K, both close to the bulk theoretical value of 71.2 emu/g. Although the saturation magnetization of magnetic nanocrystals typically exhibit a volume dependence for both shapes and sizes,^{9,15–17} the present CoFe_2O_4 spherical- or cubic-shaped nanocrystals do not exhibit much difference because of the relatively large particle sizes. However, the coercivity of the cubic nanocrystals (1980 Oe at 10 K and 200 Oe at 250 K) is somewhat smaller than that observed for the spherical nanocrystals (3000 Oe at 10 K and 500 Oe at 300 K). Figure 4 shows the field-cooled (FC) and zero-field-cooled (ZFC) magnetization curves of the spherical and cubic CoFe_2O_4 nanocrystals. Both the spherical and cubic CoFe_2O_4 nanocrystals exhibit blocking temperatures, which are somewhat above room temperature and relatively low coercivity values at room temperature are observed, as compared to the bulk.

The initial increase in the coercivity with increasing volume has been attributed to the increase in magnetic anisotropy since an applied field should be able to overcome the energy barrier and change the orientation of magnetization.

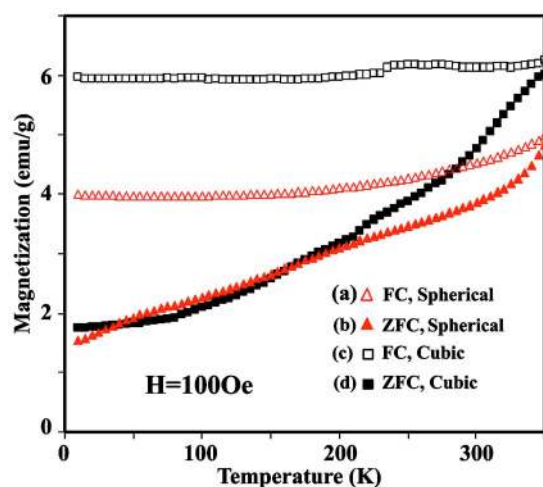


FIG. 4. (Color online) (a) FC and (b) ZFC magnetizations of spherical CoFe_2O_4 nanocrystals and (c) FC and (d) ZFC magnetizations of cubic CoFe_2O_4 nanocrystals, measured with an applied field of 100 Oe.

The subsequent decrease in the coercivity with size results from a change of the magnetization process from coherent rotation to domain wall switching.^{5,9} The coercivity has to be considered together with the surface pinning of magnetic moments and the resulting surface anisotropy,¹⁸ which can influence the dipole interaction between the neighboring nanocrystals. The surface magnetic disorder and pinning originate from missing coordinating oxygen anions around the surface metal cations. When the coordination of surface metal cations has a closer similarity to the coordination symmetry of the metal cations in the core of a nanocrystal, the surface anisotropy should be lower.¹⁹ As compared to the curved topology of spherical nanocrystals, the flat surfaces of cubic nanocrystals enable the surface metal cations to possess a more symmetric coordination with fewer missing coordinating oxygen ions. Cubic morphology nanocrystals, with an aspect ratio of almost 1, are magnetically quasi-isotropic, and, hence, magnetic shape anisotropy would not be expected to be a significant contributor. Therefore, the surface anisotropy should be smaller in cubic than in spherical-shaped nanocrystals. The cubic nanocrystals thus show a much lower coercivity than the spherical nanocrystals for the same volume.⁵ In the present study, the volume of the cubic nanocrystals is about 1520 nm^3 , which is significantly larger than the 735 nm^3 volume of the spherical nanocrystals. Therefore, the coercivity of the cubic nanocrystals is not much smaller than that of the spherical CoFe_2O_4 nanocrystals. It should be noted that the influence of the dipole interaction between the neighboring nanocrystals is basically

averaged out because of the random orientation in the powder samples.

In conclusion, shape-controlled CoFe_2O_4 nanocrystals have been obtained via thermal decomposition of an intimately mixed $\text{Co}^{2+}\text{Fe}_2^{3+}$ -oleate complex, prepared via low temperature reaction of the constituent metal halides with sodium oleate. The use of an intimately mixed binary metal-oleate precursor, with similar decomposition temperature of the constituents, is critical for the compositional and structural uniformity of the synthesized CoFe_2O_4 nanocrystals. The shape and average size of the monodisperse CoFe_2O_4 , primarily dictated by the initial concentration of the synthetic precursors, vary from $11.2 \pm 0.4 \text{ nm}$ for the perfectly spherical nanocrystals to $11.5 \pm 0.5 \text{ nm}$ for cubic nanocrystals. The saturation magnetization of the spherical and cubic CoFe_2O_4 is 72.9 and 73.3 emu/g, respectively, close to the bulk theoretical value. The coercivity of cubic nanocrystals is about 200 Oe, which is somewhat smaller (500 Oe) obtained for the spherical nanocrystals.

This work was supported by NSF under Grant No. ECS-0621850. The authors wish to thank J. W. Harrell for helpful discussions.

¹Y. Yin and A. P. Alivisatos, *Nature (London)* **437**, 664 (2005).

²M. A. El-Sayed, *Acc. Chem. Res.* **37**, 326 (2004).

³B. Y. Geng, J. Z. Ma, X. W. Liu, Q. B. Du, M. G. Kong, and L. D. Zhang, *Appl. Phys. Lett.* **90**, 043120 (2007).

⁴S. Sun, C. B. Murray, D. Weller, L. Folks, and A. Moser, *Science* **287**, 1989 (2000).

⁵A. H. Lu, E. L. Salabas, and F. Schüth, *Angew. Chem., Int. Ed.* **46**, 1222 (2007).

⁶J. Smit and H. P. J. Wijn, *Ferrites* (Wiley, New York, 1959).

⁷R. A. McCurrie, *Ferromagnetic Materials—Structure and Properties* (Academic, London, 1994).

⁸H. Zeng, P. M. Rice, S. X. Wang, and S. Sun, *J. Am. Chem. Soc.* **126**, 11458 (2004).

⁹Q. Song and Z. J. Zhang, *J. Am. Chem. Soc.* **126**, 6164 (2004).

¹⁰C. N. Chinnasamy, B. Jeyadevan, K. Shinoda, K. Tohji, D. J. Djayaprawira, M. Takahashi, R. J. Joseyphus, and A. Narayanasamy, *Appl. Phys. Lett.* **83**, 2862 (2003).

¹¹T. Hyeon, *Chem. Commun. (Cambridge)* **2003**, 927.

¹²J. Park, K. An, Y. Hwang, J. G. Park, H. J. Noh, J. Y. Kim, J. H. Park, N. M. Hwang, and T. Hyeon, *Nat. Mater.* **3**, 891 (2004).

¹³N. Bao, L. Shen, Y. Wang, P. Padhan, and A. Gupta, *J. Am. Chem. Soc.* **129**, 12374 (2007).

¹⁴Z. A. Peng and X. Peng, *J. Am. Chem. Soc.* **124**, 3343 (2002).

¹⁵X. Battle, and A. Labarta, *J. Phys. D* **35**, R15 (2002).

¹⁶C. N. Chinnasamy, B. Jeyadevan, K. Shinoda, K. Tohji, D. J. Djayaprawira, M. Takahashi, R. Justin-Joseyphus, and A. Narayanasamy, *Appl. Phys. Lett.* **83**, 2862 (2003).

¹⁷N. Moumen and M. P. Pileni, *Chem. Mater.* **8**, 1128 (1996).

¹⁸M. L. Néel, *J. Phys. Radium* **15**, 225 (1954).

¹⁹C. R. Vestal and Z. J. Zhang, *J. Am. Chem. Soc.* **125**, 9828 (2003).